J|A|C|S
COMMUNICATIONS

Published on Web 08/17/2006

Self-Coiling of $Ag_2V_4O_{11}$ Nanobelts into Perfect Nanorings and Microloops

Guozhen Shen*,† and Di Chen‡

Nanoscale Materials Center, National Institute for Materials Science (NIMS), 1-1 Namiki, Tsukuba, Ibaraki 305-0044, Japan, and Photocatalytic Materials Center, National Institute for Materials Science (NIMS), 1-2-1 Sengen, Tsukuba, Ibaraki 305-0047, Japan

Received June 12, 2006; E-mail: shen.guozhen@nims.go.jp

Direct fabrication of complex nanoarchitectures with controlled morphology, orientation, and dimensionality has attracted much attention because such control is critical in investigating the shape and structural dependence of many applications, developing new pathways for materials synthesis and new applications of nanostructured materials.[1−5]

Helical structures are the most fundamental structural configurations for proteins, RNAs, and many other biomolecules. Recently, helical structures were also observed for a number of inorganic materials: for example, ZnO nanosprings, nanospirals, nanohelixes, and nanorings,[6−10] carbon nanotube coils,[11] amorphous silica nanosprings,[12] SiC nanosprings,[13] InP nanosprings,[14] AlN nanorings and nanosprings,[15] SnO_2 rings, springs, and spirals.[16] Among these helical structures, perfect free-standing rings formed by the self-coiling of nanobelts are the most outstanding members.[6−10,15,16] However, to the best of our knowledge, all such kinds of rings are synthesized in the gas phase processes at very high temperature. No report on the solution synthesis of such self-coiled free-standing rings could be found.

In this communication, we report on the first discovery of $Ag_2V_4O_{11}$ nanorings and microloops formed by the self-coiling of $Ag_2V_4O_{11}$ nanobelts under hydrothermal process, without the use of any template or organic surfactant. The $Ag_2V_4O_{11}$ nanorings are formed by the self-coiling of one single-crystalline [30$\bar{2}$] grown $Ag_2V_4O_{11}$ nanobelt, while the microloops were formed by several nanobelts.

$Ag_2V_4O_{11}$ nanorings and microloops were synthesized in a hydrothermal process by the reaction between $AgNO_3$ and V_2O_5 powders in distilled water at 170 °C for 12 h (Supporting Information). After reaction, the structure of the obtained sample was checked using XRD. The results reveal the formation of pure monoclinic $Ag_2V_4O_{11}$ structure with lattice parameters consist with the literature.

The morphology of the sample was checked by scanning electron microscopy (SEM). A low-magnification SEM image shows that the dominant components of the synthesized sample are nanobelts with a uniform size distribution, but a significant amount of nanobelts has ring or loop shapes. The process is of high reproducibility from run to run (>90%), though the yield of nanorings and loops is relatively not very high. High-magnification SEM images of typical $Ag_2V_4O_{11}$ nanorings are shown in Figure 1a−e with different view directions. It can be seen that all the $Ag_2V_4O_{11}$ nanorings have perfect circular shape of complete rings with uniform shapes and flat surfaces. Typical nanorings have diameters of 3−5 μm and thin and wide shells with a thickness of ~30−50 nm. Composition of the formed nanorings was checked using an X-ray energy dispersive spectrometer (EDS), and the spectrum is shown in Figure 1f. It shows the presence of Ag, V, and O, confirming the formation of $Ag_2V_4O_{11}$.

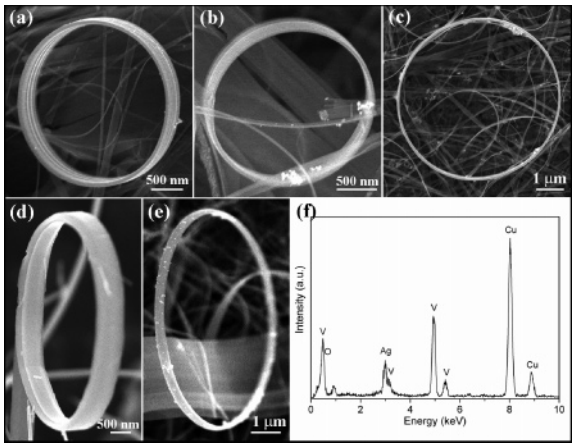

Figure 1. (a−e) Representative SEM images of the obtained $Ag_2V_4O_{11}$ nanorings. (f) EDS spectrum of the $Ag_2V_4O_{11}$ nanorings.

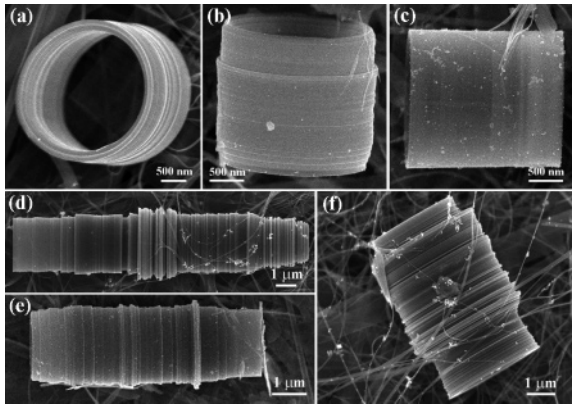

Figure 2. (a−b) SEM images of the $Ag_2V_4O_{11}$ microtube-like loops formed by rolling of nanobelts. (c−d) SEM images of the $Ag_2V_4O_{11}$ microloops by rolling of several nanobelts.

Figure 2 shows the SEM image of the synthesized $Ag_2V_4O_{11}$ microloops. Mainly two kinds of loops exist in the product. One is the microtube-like loop with uniform diameter along the whole tube (Figure 2a−c), and the other is a microloop with varied diameter (Figure 2d−f). It is noted that both the two kinds of microloops have hollow cavities as indicated in these images.

The morphology and microstructures of the interesting $Ag_2V_4O_{11}$ structures were further studied using HRTEM and selected area electron diffraction (SAED). Figure 3a shows the TEM image of a single $Ag_2V_4O_{11}$ ring with a radius of about 3 μm. The corresponding SAED pattern shown in the inset shows the single-crystal nature of the whole ring. That is to say, the complete ring is made of a single-crystalline ribbon bent evenly at the curvature of the ring.

† Nanoscale Materials Center.
‡ Photocatalytic Materials Center.

10.1021/ja064123g CCC: $33.50 **© 2006 American Chemical Society**

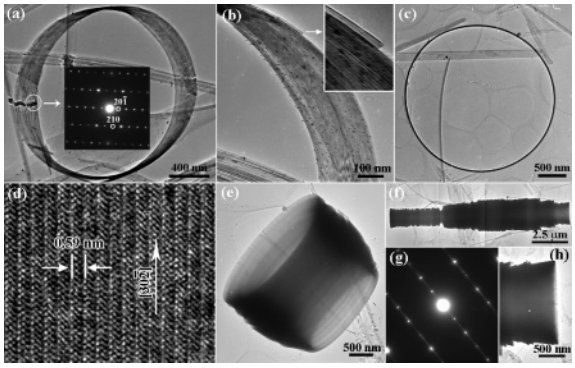

Figure 3. (a) TEM image of a single $Ag_2V_4O_{11}$ nanoring and its SAED pattern. (b) High-magnification image showing the belt morphology. (c) Top view of a single $Ag_2V_4O_{11}$ nanoring. (d) HRTEM image taken from a $Ag_2V_4O_{11}$ nanoring. (e,g) TEM image and its SAED pattern of a $Ag_2V_4O_{11}$ loop. (f) TEM image of a complex $Ag_2V_4O_{11}$ loop. (h) High-magnification TEM image of the tip of the loop in part f.

From this image, it also can be seen that, although the ring has a very large radius, its thickness is very thin at ~50 nm. The ribbon shape is clearly shown in Figure 3b. An enlarged image of the overlapping ends of the loop is shown in the inset, which suggests the possible self-coiling of a single nanobelt into rings. The extremely thin thickness of the ring can be further seen from the top-view TEM image in Figure 3c. The ring shown in this image has a radius of ~4 μm, while the thickness is thinner than 50 nm, in agreement with the SEM results. Figure 3d shows a typical HRTEM image of a single $Ag_2V_4O_{11}$ nanoring. The clear lattice image indicates the high crystallinity and single-crystalline nature of the $Ag_2V_4O_{11}$ nanoring. A lattice spacing of 0.59 nm for the $[20\bar{1}]$ plane of the monoclinic $Ag_2V_4O_{11}$ structure can be readily resolved. Combined with the SAED pattern in Figure 3a, it is clear that the as-synthesized $Ag_2V_4O_{11}$ nanoring is single crystal with the preferred orientation along the $[30\bar{2}]$ plane. TEM images of the tube-like microloop and diameter-varied microloop are shown in Figure 3e and f. The corresponding SAED pattern in Figure 3g also shows their single-crystalline nature. The streak-like contrasts in the pattern indicate the existence of stacking faults in the microloop. The hollow cavity of the microloop is clearly shown in Figure 3h.

For the growth of inorganic ring-like nanostructures in the solution process, Murray et al. proposed an oriented attachment of a nanoparticle mechanism.[17] The restructuring of polymer−inorganic hybrid nanocrystallines during mineralization and the dissolution of nanocrystals during crystal growth based on the well-known Ostwald ripening process from the inner side toward the outside is proposed to explain the formation of hexagonal ZnO nanorings.[18,19] The self-assembly of nanoparticles with an intrinsic hexagonal symmetry is suggested to explain the formation of ring-like CdS nanostructures.[20] However, we think the growth mechanism proposed in the solution process cannot be used to explain the formation of the present $Ag_2V_4O_{11}$ structures, based on our experimental results. On the other hand, previously, the loop-by-loop coaxial, uni-radius, self-coiling of a single nanobelt is used to explain the formation of nanorings, such as ZnO nanorings[6−9,21] in the vapor phase processes. Since the present $Ag_2V_4O_{11}$ rings and loops synthesized from the solution process have morphologies similar to those nanorings obtained from the vapor process, a similar mechanism may also be used in the present work. Monoclinic $Ag_2V_4O_{11}$ has a space group of $C2/m$, and the oxygen atoms around the Ag atom have 5-fold symmetry and V atoms form distorted octahedrons (Supporting Information, Figure S3a). When grown in hydrothermal process, thin, straight, polar surface-dominated $Ag_2V_4O_{11}$ nanobelts along the $[30\bar{2}]$ planes are formed first (Supporting Information, Figure S3b). The spontaneous polarization-induced electrostatic energy can decrease by self-rolling into a circular ring due to the neutralization of the dipole moment. When the spontaneous polarization-induced electrostatic energy is larger than the elasticity energy, the straight nanobelts tend to self-coil into a circle structure. To confirm the above hypothesis, the intermediate product by reaction at shorter time (5 h) was checked. From the SEM images (Supporting Information, Figure S4), the ends and the screw coiling of the $Ag_2V_4O_{11}$ nanobelts are clearly seen, accompanied by the TEM image in Figure 3b inset, verifying our proposed self-coiling growth process.

In summary, we synthesized $Ag_2V_4O_{11}$ rings and loops in a simple hydrothermal process. Both the rings and loops are formed by the self-coiling of $Ag_2V_4O_{11}$ nanobelts, which have growth directions along the $[30\bar{2}]$ direction. By varying the experimental conditions, such as using surfactants, controlling temperatures, etc., we are currently working on the improvement of the yield of the interesting $Ag_2V_4O_{11}$ rings and loops. With the improvement of yield, chemical and physical properties of these structures may be measured.

Acknowledgment. We thank Dr. C. H. Ye at the Institute for Solid State Physics, Chinese Academy of Science, for helpful discussions.

Supporting Information Available: Experimental procedures for the synthesis of $Ag_2V_4O_{11}$ rings and loops, low-magnification SEM images of the products, more SEM images of the $Ag_2V_4O_{11}$ nanorings and microloops, structure model of monoclinic $Ag_2V_4O_{11}$ with polar surfaces, and SEM images showing the self-coiling of $Ag_2V_4O_{11}$ nanobelts into rings and loops. This material is available free of charge via the Internet at http://pubs.acs.org.

References

(1) Hu, J. T.; Odom, T. W.; Lieber, C. M. *Acc. Chem. Rev.* **1999**, *32*, 435.
(2) Mbindyo, J. K. N.; Mallouk, T. E.; Mattzela, J. B.; Kratochvilova, I.; Razavi, B.; Jackson, T. N.; Mayer, T. S. *J. Am. Chem. Soc.* **2002**, *124*, 4020.
(3) Yuan, J. K.; Li, W. N.; Gomez, S.; Suib, S. L. *J. Am. Chem. Soc.* **2005**, *127*, 14184.
(4) Liu, B.; Zeng, H. C. *J. Am. Chem. Soc.* **2004**, *126*, 8124.
(5) Lao, J. Y.; Wen, J. G.; Ren, Z. F. *Nano Lett.* **2002**, *2*, 1287.
(6) Kong, X. Y.; Wang, Z. L. *Appl. Phys. Lett.* **2004**, *84*, 975.
(7) Kong, X. Y.; Wang, Z. L. *Nano Lett.* **2003**, *3*, 1625.
(8) Yang, R. S.; Ding, Y.; Wang, Z. L. *Nano Lett.* **2004**, *4*, 1309.
(9) Kong, X. Y.; Ding, Y.; Yang, R. S.; Wang, Z. L. *Science* **2004**, *303*, 1348.
(10) Gao, P. X.; Ding, Y.; Mai, W. J.; Hughes, W. L.; Lao, C.; Wang, Z. L. *Science* **2005**, *309*, 1700.
(11) Amelinckx, S.; Zhang, X. B.; Bernaerts, D.; Zhang, X. F.; Ivanov, V.; Nagy, J. B. *Science* **1994**, *265*, 635.
(12) Zhang, H. F.; Wang, C. M.; Buck, E. C.; Wang, L. S. *Nano Lett.* **2003**, *3*, 577.
(13) Zhang, H. F.; Wang, C. M.; Wang, L. S. *Nano Lett.* **2002**, *2*, 941.
(14) Shen, G. Z.; Bando, Y.; Zhi, C. Y.; Yuan, X. L.; Sekiguchi, T.; Golberg, D. *Appl. Phys. Lett.* **2006**, *88*, 243106.
(15) Duan, J.; Yang, S.; Liu, H.; Gong, J.; Huang, H. B.; Zhao, X. N.; Tang, J.; Zhang, R.; Du, Y. W. *J. Cryst. Growth* **2005**, *283*, 291.
(16) Yang, R. S.; Wang, Z. L. *J. Am. Chem. Soc.* **2006**, *128*, 1466.
(17) Cho, K. S.; Talapin, D. V.; Gaschler, W.; Murray, C. B. *J. Am. Chem. Soc.* **2005**, *127*, 7140.
(18) Li, F.; Ding, Y.; Gao, P. X.; Xin, X. Q.; Wang, Z. L. *Angew. Chem., Int. Ed.* **2004**, *43*, 5238.
(19) Peng, Y.; Xu, A. W.; Deng, B.; Antonietti, M.; Colfen, H. *J. Phys. Chem. B* **2006**, *110*, 2988.
(20) Liu, B.; Zeng, H. C. *J. Am. Chem. Soc.* **2005**, *127*, 18262.
(21) Hughes, W. L.; Wang, Z. L. *J. Am. Chem. Soc.* **2004**, *126*, 6703.

JA064123G